PHASE DIAGRAM STUDIES OF BINARY HYDROCARBON SYSTEMS FOR A FREEZING DESALINATION PROCESS

by

PETER SHENG-SHYONG MAA

B. S., National Taiwan University, 1964

A MASTER'S THESIS

submitted in partial fulfillment of the

requirements for the degree

MASTER OF SCIENCE

Department of Chemical Engineering

KANSAS STATE UNIVERSITY
Manhattan, Kansas

1968

Approved by:

Liang Sheng Fan

Major Professor

TABLE OF CONTENTS

LIST OF FIGURES

LIST OF FIGURES--Continued

LIST OF TABLES

INTRODUCTION

Freezing Desalination Process

"One of the newest-and potentially most promising-of the desalination processes is that of freezing (1)". In all of the important freezing processes, the refrigerant (working medium) comes into direct contact with the sea water brine when ice is being formed.

There are three important freezing processes:

(1) The Carrier and Fairbanks Whitney Process: the refrigerant is the water itself. Vapor and liquid phases are involved.

(2) The process developed by Blaw-Knox, Struthers Scientific, and North American Avaiation: the refrigerant is a light hydrocarbon or other refrigerant. Vapor and liquid phases are involved.

(3) The process invented by the Chengs (2): it is based on the freezing point inversion due to applied pressure. Hereafter, it will be called the inversion freezing process, the refrigerant is a heavy hydrocarbon or other refrigerant. Solid and liquid phases are involved.

In the inversion process, distinguished from the conventional freezing process, only the condensed phases (liquid and solid) are involved. This has a considerable effect on the energy requirements of the process and simplifies the control of ice crystallization.

Inversion Freezing Process

The feasibility of this process is based on the normal melting characteristics of water under different levels of pressure. This

characteristic is shown in Figure A-1 (3). Water melts at a lower temperature under a higher applied pressure, that is,

$$(dP/dT)_{melting} < 0,$$

while a binary hydrocarbon system melts at a higher temperature under a higher applied pressure, that is,

$$(dP/dT)_{melting} > 0,$$

Due to this difference, a substance which will melt at a temperature lower than the freezing point of an aqueous solution may melt at a temperature higher than the melting point of water when a sufficiently high pressure is applied.

This process can be divided into the low-pressure phase transformation and the high-pressure phase transformation. The low-pressure phase transformation takes place according to the following equation:

$$\text{Sea Water } (c_1) + \text{Organic Slurry} \longrightarrow \text{Ice} + \text{Brine } (c_2) + \text{Organic Liquid}$$

The organic slurry melts, and ice freezes from sea water. The mass of ice entrains some of the brine from which it is formed. The salt content in brine c_2 is greater than the salt content in sea water c_1. Ice is then separated from the brine and organic liquid and washed, and the organic liquid is recovered. Both ice and organic liquid are transported to an ice melter for the high-pressure operation. In the low-pressure operation, heat is transferred from the sea water to the organic slurry.

The high-pressure phase transformation takes place according to the following equation:

$$\text{Ice} + \text{Organic Liquid} \longrightarrow \text{Fresh Water} + \text{Organic Slurry}$$

Here the ice completely melts and the organic liquid partially freezes. The organic solid is suspended in the organic liquid, forming the organic slurry. Heat is transferred from the direction of the organic liquid to the ice. The organic slurry will be reused in the low-pressure phase transformation. Hence, a limited amount of refrigeration is needed in this process. Four condensed phases are involved in the high-pressure phase transformation, namely, ice, an organic liquid, water, and an organic solid. The organic liquid is contacted with ice in the high-pressure ice melter and the mixture is pressurized sufficiently so that the required transformation takes place.

The melting point decrease of ice under the applied pressure is shown in Table A-1 in the appendix (4). This is also plotted in Figure A-2.

No high-pressure data of binary hydrocarbon systems are available. The purpose of this work was to devise a calorimeter to study the phase behavior of some of the binary hydrocarbon systems under high pressures and to determine the pressure to be applied for this inversion freezing process.

REVIEW OF LITERATURE

Low-Pressure Techniques and Data

Techniques for the determination of solid-liquid equilibrium temperatures at atmospheric pressure were described by Weissberger (5), Farkas (6), Fox (7), Stull (8), Aston (9), Ziegler, et al. (10), Ruehrwein, et al. (11), Tilicheev, et al. (12), Finks, et al. (13), Salzgeber (14), Tunnicliff (15), Aranow, et al. (16), Vassallo (17), etc. All the techniques are briefly summarized in the following.

In Weissberger's book (5), the various methods for determining melting and freezing temperatures have been classified into six categories, four for pure or nearly pure substances and the other two for binary mixtures. A list of the more important applications and the estimated maximum accuracy of each are given as a guide for selection of methods for determining melting and freezing temperatures.

In Farkas' book (6), only the most precise methods were discussed. These were the dynamic, time-temperature method, and the static, calorimetric method.

Dynamic Time-Temperature Method

The method of Schwab and Wichers (18), which is one of the most precise of the time-temperature techniques, has the serious disadvantage that in the course of the measurement the purity of the sample is destroyed. Other procedures of high precision are those of Smittenberg, et al. (19) and Skau (20). However, since the technique developed by Rossini, et al. (21) at the National Bureau of Standards has been subjected to considerable testing, it will be discussed rather than the other methods.

In common with other time-temperature methods, the technique of Rossini, et al. (21) employs a constant heat-leak, controlled and adjusted in this case by means of an evacuable Dewar, to cool and freeze (or heat and melt) the sample. In addition, the use of a constant-speed stirring mechanism and of large thermal heads between the refrigerant and the sample ensures a constant cooling rate which is essential to the precision of the method. Specially designed basket or spiral-type stirrers are used for ensuring efficient contact between the liquid and the solid phases to promote the attainment of thermodynamic equilibrium. Precise temperature measurements ($\pm$0.001 ^{o}C) are made with platinum resistance thermometers. For materials which have a tendency to supercool, it is relatively simple to induce crystallization by appropriate seeding. After the crystallization has begun, the temperature of the sample is recorded at definite time intervals. During the cooling period, just before the crystallization begins, the time is recorded at fixed temperature intervals. While the freezing is going on, the stirring is continued until the crystallization has reached the point where the stirrer begins to labor. At that point, both the stirring and the temperature measurements are stopped. For those samples which do not approach equilibrium readily on freezing, the melting point is determined instead. The apparatus and technique for this method have been carefully described in numerous publications by Rossini to which the reader may refer for further details.

Static Adiabatic Calorimeter Method

The second general method for the determination of the melting point is a static calorimetric technique. In marked contrast with the time-

temperature procedure in which the rate of change of the temperature is measured, in the calorimetric procedure great care is taken to measure the temperature at equilibrium conditions.

In addition to the precise determination of the "100% melted" temperature, the calorimetric technique has the advantage that the heat of fusion and the triple point for zero impurity can be determined in the same series of measurements. The determination of the heat of fusion in a calorimeter is the most accurate method of measuring that thermodynamic quantity. When a triple point is determined in a calorimeter, one is also able to measure the heat capacity of the solid below the melting point with very little additional effort.

Recently, special calorimeters have been designed primarily to determine triple points and purities of hydrocarbons (22, 23). The design of these new calorimeters has been based on that of the precision instruments, but modifications have been introduced which will permit rapid operation by only one individual. Figure 1 is a schematic drawing of such a triple-point calorimeter. One major departure from the precision instruments is the large tube which connects the calorimeter with the vacuum system and through which the sample is introduced. In conventional design, these filling tubes are always as small as possible so as to reduce the heat leak to and from the calorimeter proper. While such narrow tubes necessitate slow distillations for filling and emptying, with large filling tubes it is possible to introduce the sample (some 15 ml.) into the calorimeter by simply pouring it down a funnel inserted into the filling tube. When the measurements are completed and the sample is to be withdrawn, it is a simple matter to slip another tube down inside the large filling tube and remove the sample by siphoning. To

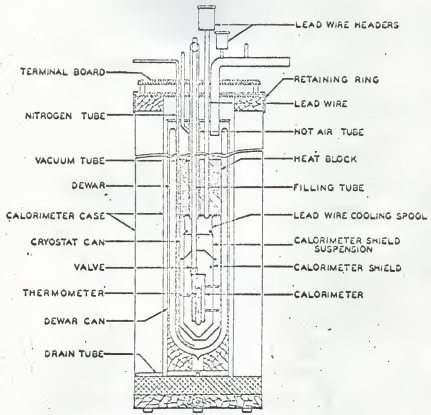

Fig. 1. Schematic drawing of calorimeter assembly. (from Farkas (6))

increase the strength and ruggedness of the assembly, the calorimeter and shields are spaced apart by means of the wooden pegs shown in Fig. 1. To reduce the heat exchange between the calorimeter and shields along these pegs, the contacts are machined to fine points. Using fewer control points and through the development of semiautomatic controls, the operation of these triple-point calorimeters is simple and straightforward. The use of continuous electronic controls (22) materially increases the precision which can be attained in these units as compared with the earlier manually-operated model (23).

In the determination of the triple point of a substance by means of the calorimetric technique, one of the most important points is to be certain that the sample has been completely crystallized before beginning the measurements. When this has been accomplished, the temperature of the sample is adjusted to the range at which measurements are to be started. In an adiabatic calorimeter, such as the triple-point calorimeters, the procedure is to maintain the temperature difference between the calorimeter (sample container) and its surrounding shields and the filling tube so small that there will be negligible interchange of heat. With the electronic controls set to maintain this temperature difference within the necessary range, the temperature of the calorimeter is followed as a function of time by means of the platinum resistance thermometer in the reentrant well.

A comparison of the time-temperature and adiabatic calorimetric results has also made in Farkas's book (6). In Fox's book (7), both calorimetric methods and noncalorimetric methods have been described for the determination of thermal properties.

Stull (8) constructed a calorimeter for small amounts of organic liquids which would enable measurements of specific heats and heats of transition to be made in the range 100 to 320 ^{o}K.

Aston and Eidinoff (9) designed a calorimeter. The calorimeter itself is similar to that of Southard and Brickwedde (24). This calorimeter is superior to any others designed for condensed gases.

Ziegler, et al. (10) designed a calibrated heat conduction calorimeter; it is a modification of Andrews' calibrated, heat-conduction calorimeter (25).

Ruehrwein, et al. (11) designed a cryostat and calorimeter. It is similar to that described by Blue and Hicks (26) except that a simpler device is employed to transfer heat from the calorimeter during the cooling operation.

Tilicheheev, et al. (12) designed a cylindrical Dewar flask and a spherical Dewar flask for thermal analysis. The cryoscopic constants and transition points of n-hexane to n-Eicosane were reported.

Finke, et al. (13) used Ruehrwein's apparatus to measure the thermal data of nine normal paraffin hydrocarbons from octane to hexadecane. Thermal data of melting points, molal heat capacities, heats of fusion, cryoscopic constants, molal heats of transition and transition temperatures, and entropy were reported.

Salzgerber (14) used Tilicheev, et al.'s technique to measure the phase diagrams of three binary hydrocarbon systems, namely, n-dodecane and n-tridecane, n-tridecane and n-tetradecane, and n-tetradecane and n-pentadecane. Three phase diagrams were reported.

Tunnicliff and Stone (15) described a calorimeter and radiation shield assembly. It was designed for spectroscopic investigations.

Aranow, et al. (16) made an analysis of the high entropy of fusion of long chain paraffins, attributing that entropy to the onset at melting of freedom of the molecule to undergo hindered rotation about each carbon to carbon bond. The theoretical results are compared with the experimental observations. The entropy of fusion of heavy paraffins yields information concerning the rotational energy levels of the molecules. An empirical relationship was stated connecting the energy levels of the molecule with the melting temperature of the molecule.

Vassallo, et al. (17) presented a differential thermal analysis method for the precise, semiautomatic determination of phase transition temperatures. Several DTA (Differential Thermal Analysis) methods were compared for estimating transition temperatures. The effects of variation in termocouple position and gage, and in heating rate were given. A recommended procedure gives a precision of ± 0.3 °C for 2- to 5-mg. samples over the temperature range from -150 to +450 °C. Liquid or solid samples were tested directly; gases, after condensation into cooled tubes within the apparatus. Conventional melting point capillary tubes were used in the simultaneous determination of melting, boiling, and inversion temperatures of organic materials.

High-Pressure Techniques and Data

Techniques for the determination of thermal data at high pressure were described by Bridgman (27), Cutler, et al. (28) and Nelson, et al. (29). They are summarized briefly in the following, and some thermal data are reprinted for the further application.

Bridgman (27) utilized a flexible bellows with attached slide-wire for the measurement of volume changes, and the changes in the resistance of a coil of manganin wire for the measurement of pressure changes.

In Cutler, et al.'s (28) work, isothermal compressions were measured for thirteen high-purity liquid hydrocarbons and two binary mixtures of liquid hydrocarbons. These hydrocarbons have a molecular weight range of 170 to 351 and included normal paraffins, cycloparaffins, aromatics, and fused ring compounds. The pressure range for these measurements was from atmospheric to as high as 10,000 bars, being limited to lower values for same compounds to avoid possible solidification of the liquid. The volume changes due to pressure were measured at six temperatures spaced about equally in the range 37.8 ^{o}C to 135.0 ^{o}C. The volume changes and pressures were measured by methods similar to those of Bridgman (27). The technique used for detection and measurement of the volume change was a modification of the Bridgman (27) bellows technique. It was call piezometer (28). The piezometer held approximately five cubic centimeters of the hydrocarbon being studied. Isothermal compressions have been studied for 13 hydrocarbons and two binary mixtures (28).

Nelson, et al. (29) investigated first order phase transitions for n-nonane, n-dodecane, n-tridecane, n-pentadecane, n-octadecane, and n-tetracosane, at pressure up to 10 kilobars and temperature up to 135 ^{o}C. By a modification of standard pizometric techniques (28), phase transition pressures, as well as the associated isothermal, isobaric volume changes were determined at approximately 25 ^{o}C intervals. Correlations established between the melting temperatures and the specific volume changes associated with phase transitions and the n-paraffin chain lengths show a strong dependence upon whether the n-paraffin is of odd or even species. This dependence becomes more pronounced at higher

pressures. The specific volume, enthalpy, and entropy changes showed no dependence upon chain length at the same melting temperature. Tables 1 and 2 are reprinted from Tables I and II of Nelson, et al.'s paper. Table 1 shows the smoothed transition pressures and the slopes of the transition curves. Table 2 shows the thermodynamic variables of first-order phase transitions in n-paraffins.

Table 1. The smoothed transition pressures and the slopes of the transition curves. Atmospheric pressure transition temperatures, when obtained from the literature are referenced accordingly. (from Nelson (29))

Compound	Type of transition	Temperature (°C)	Pressure (bars)	(dP/dT) (bars/°C)
$n\text{-}C_9$	Liquid-	-53.5[a]	1	74.6
	solid I	15.56	4805	87.8
	Solid I	...	1	...
	solid II	15.56	4965	
	Liquid-	37.78	6795	94.9
	solid II	60.00	9030	105.5
$n\text{-}C_{12}$	Liquid-	-9.5[b]	1	43.1
	solid	15.56	1175	49.9
		37.78	2390	57.0
		60.00	3775	65.7
		79.44	5155	74.7
		98.89	6712	86.1
		115.00	8192	98.9
$n\text{-}C_{13}$	Liquid-	-5.3[c]	1	42.5
	solid I	15.56	1050	55.5
	Solid I-	-17.9	1	41.1
	solid II	15.56	1442	45.7
	Liquid-	37.78	2430	67.4
	solid II	60.00	4040	77.6
		79.44	5605	84.6
		98.89	7310	90.9
$n\text{-}C_{15}$	Liquid	9.9[b]	1	45.1
	solid I	15.56	280	47.7
		37.78	1400	55.1
	Solid I-	-2.0	1	38.1
	solid II	15.56	704	41.6
		37.78	1664	46.8
	Liquid-	60.00	2735	64.0
	solid II	79.44	4075	73.5
		98.89	5615	84.7
		115.00	7055	96.0
		135.00	9115	114.0
$n\text{-}C_{18}$	Liquid-	27.8[b]	1	38.4
	solid	37.78	400	41.5
		60.00	1408	49.0

Table 1. The smoothed transition pressures and the slopes of the transition curves. Atmospheric pressure transition temperatures, when obtained from the literature are referenced accordingly. (from Nelson (29))

Compound	Type of transition	Temperature (°C)	Pressure (bars)	(dP/dT) (bars/°C)
$n\text{-}C_{18}$ (continued)	Liquid-solid	79.44	2450	56.6
		98.89	3620	64.0
		115.00	4705	70.7
		135.00	6220	79.9
$n\text{-}C_{24}$	Liquid-solid I	50.3[c]	1	39.6
		60.00	405	41.8
	Solid I-solid II	48.1[c]	1	41.9
		60.00	416	41.9
	Liquid-solid II	79.44	1270	46.9
		98.89	2260	53.7
		115.00	3175	60.7
		135.00	4508	72.2

[a] F. D. Rossini et al., Selected Values of Physical and Thermodynamic Properties of Hydrocarbons and Related Compounds, American Petroleum Institute Project 44 (Carnegie Press, Pittsburgh, Pennsylvania, 1953).
[b] R. W. Schiessler and F. C. Whitmore, Ind. Eng. Chem. 47, 1660 (1955).
[c] P. R. Templin, Ind. Eng. Chem. 48, 154 (1956).

Table 2. The thermodynamic variables of the first-order phase transition in n-paraffins (from Nelson (29))

Compound	Type of transition	Temperature (°C)	ΔV (cm^3/g)	ΔH (cal/g)	ΔU (cal/g)	ΔS (cal/g °K)
$n\text{-}C_9$	Liquid-	-53.5[a]	0.0737	28.83	28.83	0.131
	solid I	15.56	0.0759	45.97	37.26	0.159
	Solid I-	...	...	...	...	...
	solid II	15.56	0.0172	...	...	...
	Liquid-	37.78	0.0714	50.34	38.75	0.162
	solid II	60.00	0.0696	58.45	43.43	0.175
$n\text{-}C_{12}$	Liquid-	-9.5[b]	0.1826	49.55	49.55	0.188
	solid	15.56	0.1510	51.99	47.75	0.180
		37.78	0.1272	53.85	46.59	0.173
		60.00	0.1098	57.44	47.54	0.172
		79.44	0.0977	61.47	49.44	0.174
		98.89	0.0862	65.99	52.17	0.177
		115.00	0.0771	70.72	55.63	0.182
$n\text{-}C_{13}$	Liquid-	-5.3[b]	0.1283	34.90	34.90	0.130
	solid I	15.56	0.1001	38.31	35.80	0.133
	Solid I-	-17.9	0.0348	8.72	8.72	0.034
	solid II	15.56	0.0421	13.27	11.82	0.046
	Liquid-	37.78	0.1188	59.48	52.59	0.191
	solid II	60.00	0.0948	58.56	49.41	0.176
		79.44	0.0832	59.30	48.16	0.168
		98.89	0.0710	57.37	44.97	0.154
$n\text{-}C_{15}$	Liquid-	9.9[b]	0.1292	40.02	40.02	0.141
	solid I	15.56	0.1211	39.84	39.03	0.138
		37.78	0.0966	39.54	36.31	0.127
	Solid I	-2.0	0.0393	9.70	9.70	0.036
	solid II	15.56	0.0392	11.25	10.59	0.039
		37.78	0.0395	13.73	12.16	0.044
	Liquid-	60.00	0.1127	57.41	50.05	0.172
	solid II	79.44	0.0949	58.77	49.53	0.166
		98.89	0.0803	60.45	49.68	0.162
		115.00	0.0708	63.04	51.11	0.162
		135.00	0.0619	68.81	55.33	0.169
$n\text{-}C_{18}$	Liquid-	27.8[b]	0.1953	53.95	53.95	0.179
	solid	37.78	0.1800	55.48	53.76	0.178
		60.00	0.1456	56.82	51.92	0.170
		79.44	0.1249	59.56	52.25	0.168
		98.89	0.1090	62.00	52.57	0.166
		115.00	0.0994	65.18	54.01	0.167
		135.00	0.0901	70.19	56.80	0.172

Table 2. The thermodynamic variables of the first-order phase transition in n-paraffins (from Nelson (29))

Compound	Type of transition	Temperature (°C)	ΔV (cm^3/g)	ΔH (cal/g)	ΔU (cal/g)	ΔS (cal/g °K)
$n\text{-}C_{24}$	Liquid-	50.3[c]	0.1215[c]	37.18	37.18	0.115
	solid I	60.00	0.0975	32.45	31.51	0.097
	Solid I-	48.1[c]	0.0662[c]	21.29	21.29	0.066
	solid II	60.00	0.0851	28.38	27.53	0.085
	Liquid-	79.44	0.1465	57.89	53.45	0.164
	solid II	98.89	0.1237	59.06	52.37	0.159
		115.00	0.1127	63.43	52.88	0.163
		135.00	0.1037	73.01	61.85	0.179

[a] F. D. Rossini et al., Selected Values of Physical and Thermodynamic Properties of Hydrocarbons and Related Compounds, American Petroleum Institute Project 44 (Carnegie Press, Pittsburgh, Pennsylvania, 1953).
[b] R. W. Schiessler and F. C. Whitmore, Ind. Eng. Chem. 47, 1660 (1955).
[c] P. R. Templin, Ind. Eng. Chem. 48, 154 (1956).

EXPERIMENTAL

Selection of a Refrigerant

An ideal refrigerant for desalination should have the following qualities: nontoxicity, a very low solubility in water, a proper melting range, a large value for the latent heat of fusion, a high $(dT/dP)_{melting}$ value, no hydrate formation, low cost and ready availability. A mixture of hydrocarbons can meet all of the above requirements (2).

N-tridecane, n-tetradecane, and n-pentadecane were studied in this work. A sample of technical grade (minimum purity of 95 mole percent) n-pentadecane was obtained from South Hampton Company. Samples of pure grade (minimum purity of 99 mole percent) n-tridecane and n-tetradecane and technical grade n-tridecane and n-tetradecane were obtained from the Phillips Petroleum Company.

Development of Experimental Technique

In the early part of this work the freezing point of a hydrocarbon mixture was measured by the "capillary tube method (5)", which is a very convenient method for measuring a eutectic type solution. However, detection of the starting and the end point of the transition region by the capillary method was difficult. This method indicated only the approximate location of the solid-liquid transition of a solid solution. Its reproducibility was generally poor. Furthermore, it was impossible to use this in a high-pressure investigation.

The next method used for measuring the freezing point was the stirring method. In this the organic solution and an equal amount of salt water (20 wt. % of salt) were mixed together by placing them in a vessel with a reciprocal motion paddle in it. The vessel was wrapped

with a cooling coil in which a coolant (antifreeze solution) was pumped. A cooling curve and a heating curve could be obtained within 30 minutes. Reasonably good data were obtained using this method at one atmosphere pressure. Because of a technical difficulty (leakage problem) at high pressure, this method has been discarded in this work. If this method could be used in a desalination plant, measurement of the physical properties could be performed within 30 minutes.

A way of using a equipment of a "magnedash" (30) to mix the organic solution in an autoclave was devised, but because the required instrument is fairly expensive, it was not tried.

The method finally used was a static method, namely, the adiabatic calorimeter method.

Experiment

The experimental equipment was designed to permit the conditions necessary to obtain reasonable data. The principal piece of equipment devised was a cell, which functioned as a calorimeter. This cell was constructed in such a way as to maintain the solid-liquid equilibrium during the heating process. The other pieces of equipment and instruments served to cool, to heat, to apply the desired pressure, and to record the temperature of the cell. A list of the equipment and instruments associated with the heating process (see Figure 2) is presented below.

Constant Temperature Bath.

This bath was made by Forma Scientific Inc., Model No. 2095. It was designed to hold close temperature control from -18 ^{o}C to +50 ^{o}C in an ambient of 24 ^{o}C. Heat was provided by a 650-watt stainless steel immersion heater located under the pump shelf. Refrigeration was supplied

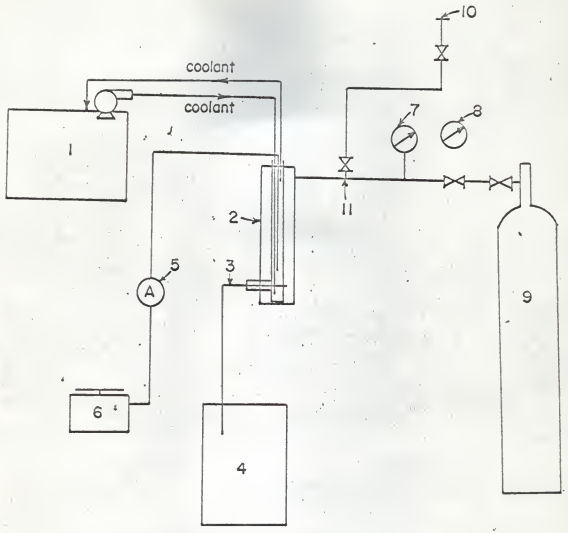

Fig. 2. Flow sheet of equipment for measuring heating curve.

(1) Constant temperature bath. (2) High pressure cylinder assembly. (3) Thermocouple. (4) Honeywell electronik 19 temperature recorder. (5) Ammeter. (6) Adjustable transformer. (7) & (8) Pressure gages (9) Nitrogen gas cylinder. (10) Compressed air source. (11) Vent or compressed air entrance.

by a copper cooling coil also located under the pump shelf and this was powered by a 1/5 HP refrigeration unit designed for continuous duty. Close control was achieved by use of a transistorized control panel operating in conjunction with a magnetic thermoregulator which provided a rapid cycle between heat and cool. Commercial anti-freeze was used as a coolant. The capacity of the bath was about eight gallons. The constant temperature bath was set at -18 °C. It was used to supply the coolant to cool the cell to the desired temperature.

High-Pressure Cylinder Assembly.

The high-pressure cylinder assembly served as a calorimeter. It was a modification of Tilicheev's (12) calorimeter. Figure 3 is an exploded view showing internal construction of the instrument, hereafter called the calorimeter. The calorimeter held approximately 250 cubic centimeters of the hydrocarbon being studied. Various components of the calorimeter are described below.

1) Cylinder. It was made of a 6 inches long stainless steel pipe. Its O. D. was 2.250 inches and its I. D. was 2 inches.

2) Center Assembly. The center pipe (see Figure 4) was a brass tube 7 inches long. Its O. D. was 0.75 inch and I. D. was 0.625 inch. The upper end was connected with a heavy disc with a thickness of 1 inch. There was a hole in the side of the disc which served as a high-pressure nitrogen inlet. An O-ring was provided at the bottom of the heavy disc.

   A number of brass discs extended from the center pipe. The brass discs (see Figure 4) were made of thin brass sheets with a thickness of 0.003 inch and O. D. of 2 inches. They

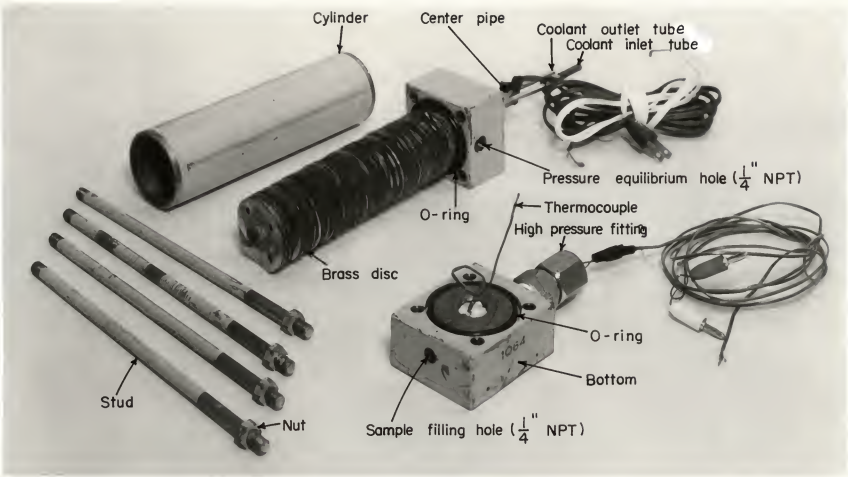

Fig. 3. Calorimeter. Exploded view showing internal construction.

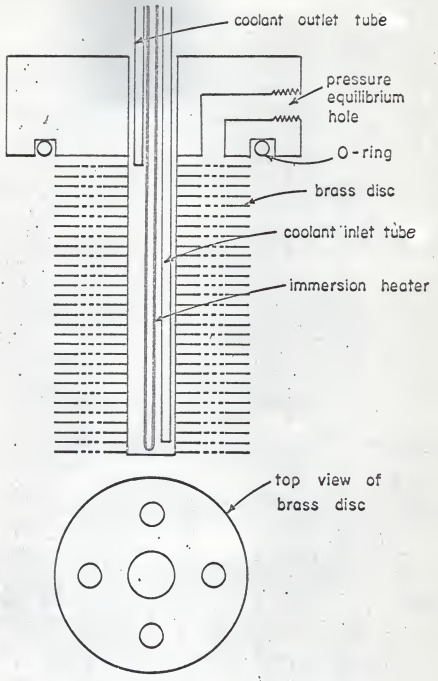

Fig. 4. Schematic view of the center assembly.

were equally spaced. The space between two neighboring discs was 1/16 inch. There were 4 holes in each disc, one for installing a thermocouple, the other three for interconnecting the solution in the system.

A plastic protector was placed on the junction of the thermocouple to prevent it from direct contact with the brass discs.

The bottom of the pipe was welded.

Two small diameter brass tubes and an electric heater were inserted inside the center pipe. One tube served as the inlet for the coolant. Its end was placed near the bottom of the center pipe in order to get good circulation of the coolant. The other tube served as the exit for the coolant. The heater was of the commercial immersion type with 46 ohms resistance.

3) Bottom. The bottom was made of 1" thick stainless steel disc. There were two holes in the opposite sides of the disc (see Figure 3). One was 0.25" NPT. It served as the sample filling hole. The other one was a 0.5 inch NPT and a thermocouple with a high-pressure fitting was installed in it.

The assembly was set up by connecting the center assembly and bottom with the cylinder with four studs and eight nuts.

Thermocouple.

The thermocouple wire was obtained from the Thermo-Electric Company and was type P-22-DT. It was 22 B & S gage solid copper and constantan wire with polyvinyl insulation. The thermocouple was made from the

specified wire and was soldered to form the junction. The ice point thermocouple was also made from the same wire. The network of the thermocouple junctions was shown in Figure 5. One thermocouple was then calibrated against a Beckman thermometer in the range of 0 °C to 5 °C. The conversion tables for thermocouples of Leeds & Northrup Company, Catalog No. 077989, Issue 2 was used to convert the potential to temperature. They agreed to each other within the limit of ± 0.004 °C. By assuming the thermocouple potential was linear in this range of operating temperature (-10 °C to + 10 °C), the conversion table could be used without further calibration (see Appendix C).

Ice Bath.

The capacity of the dewar flash was 200 ml. The thermocouple probe was made by the Thermo Electric Company, Catalog No. 5-D-0811-S. It had a diameter of 1/16 inch, bushing size of 1/8 inch, immersion length of 4 inches, and was without lead.

About 200 cubic centimers of small ice particles (about 1/4 inch diameter) were put in the dewar flask. The ice was replenished and firmly packed and water was drawn off in order to get a constant temperature at 0 °C. It served as a reference temperature.

Potential Recorder.

The instrument used was a Honeywell Two-Pen Electronik 19* Lab Recorder. It provided two continuous balance potentiometers in a small and compact package. Each measuring system of the recorder simultaneously measured, recorded, and indicated the value of an input variable. It provided high-speed response, quick selection of multiple spans (from 100

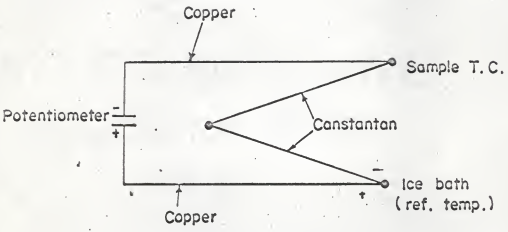

Fig. 5. Thermocouple connections.

microvolts to 100 volts), positive and negative zero rangeability, and selection of multiple chart speeds (10 fixed speeds). A span of 0.5 millivolt was used throughout the experiment. The accuracy was within 1.25 microvolt, that is, about 0.03 ^{o}C.

The 6-inch calibrated width chart was used. It was evenly graduated in percent -2 to +102 reading from right to left.

Ammeter.

A Weston model 528 ammeter was used to measure the heat input. It could measure the current to an accuracy of 0.1 ampere.

Adjustable Transformer.

The current of heat input was adjusted by an adjustable transformer. It was made by Standard Electrical Products Company. It was of type 25208 with the maximum output 2.8 KVA.

Nitrogen Gas Cylinder.

It was used to pressurize the system. The maximum pressure of the cylinder was 2500 psig.

Pressure Regulator.

It was used to regulate the pressure of the calorimeter. It consisted of two pressure gages, one rubber tube, and a regulating valve. The front pressure gage was for indicating the pressure of the Nitrogen Cylinder. The rear pressure gage was for indicating the pressure of the calorimeter.

Operating Procedures

1) The constant temperature bath was set at -18 °C, so that the coolant was at the same temperature as the set point.
2) A pipette was used to put 200 cubic centimeters of hydrocarbon solution with a known composition in the calorimeter.
3) The insulation material (asbestos rope & glass wool) was put on the calorimeter.
4) The circulation pump was turned on to cool the whole system. When the temperature reached about 8 °C below the solid-liquid transition region, the pump was turned off.
5) The whole system was heated by adding a small amount of heat.
6) The zero point of the potential recorder was adjusted. The recorder was used to record the heating history of the system. Such measurements and energy additions were continued into and through the fusion region until all the pertinent data had been obtained. A curve was recorded on the chart.
7) The mixture was cooled again.
8) The nitrogen cylinder was opened and the valve was adjusted to get the desired pressure.
9) Repeat Step 5.
10) The pressure was released by opening the vent.
11) In case that the composition were different from run to run, about 20 cubic centimeters of benzene were put into the calorimeter. The calorimeter was shaken and then the solution was poured out. The calorimeter was then connected to a high-pressure air source (70 psig) to blow the calorimeter for about one hour, in order to get a dry, clean calorimeter for the next run.

RESULTS AND DISCUSSION

The organic solutions used were prepared from the hydrocarbons previously specified. A 250 cubic centimeters volumetric cylinder (division 2 cubic centimeters) was used to make the solutions. Three different binary systems were measured and six phase diagrams were obtained. A number of runs were made using a 70-30 (volume %) mixture of n-tridecane and technical grade n-pentadecane, in order to test the precision (reproducibility) of the equipment. The melting point of distilled water was also measured in order to test the acuracy of the calorimeter.

Figure 6 shows the solid-liquid equilibrium phase diagrams of the n-tridecane (pure grade) and n-tetradecane (pure grade) binary system, which was plotted from data in Table 3. The circles represent the phase behavior at a pressure of 110 atmospheres and the crosses represent the phase behavior at a pressure of 1 atmosphere. The melting points and the freezing points in Table 3 were obtained from Figures C-1, C-2, C-3, C-4, C-5, and C-6 in Appendix C which are the heating curves of n-tridecane and n-tetradecane mixturews with different compositions.

The chart speed of the potentiometric recorder used for recording the heating curves was 10 min/in. The heat input rate was 41.3 cal/min. For each mixture, heating curves obtained at 110 atmospheres and at 1 atmosphere were recorded on the same figure for comparison.

Figure 7 shows the solid-liquid equilibrium phase diagrams of the technical grade mixture of n-tridecane and n-pentadecane. The circles represent the phase behavior at a pressure of 103 atmospheres and the crosses represent the phase behavior at a pressure of 1 atmosphere. This was plotted from Figures C-7, C-8, C-9, C-10, C-11 and C-12 in Appendix C. No experiment at a composition near pure n-pentadecane was carried out. Therefore, the curves were extrapolated as shown in the figure.

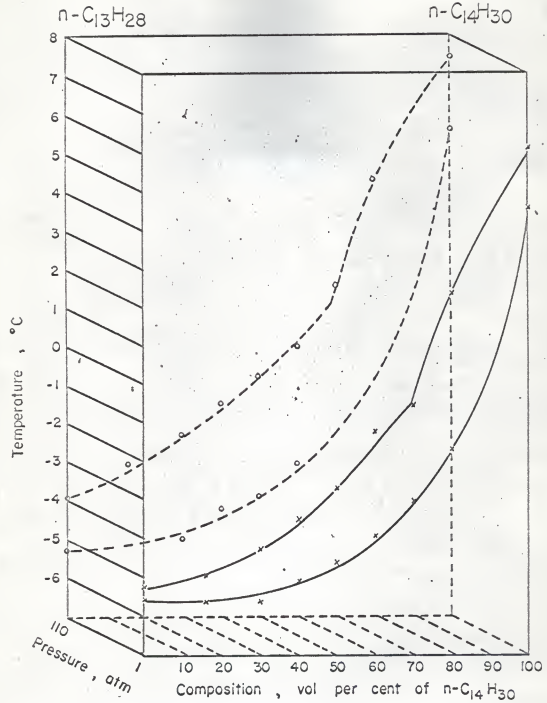

Fig. 6. Phase diagrams of n-tridecane (pure grade) and n-tetradecane (pure grade) binary system.

Table 3. Freezing points and melting points for different compositions of a mixture of n-tridecane (pure grade) and n-tetradecane (pure grade) at 1 atmosphere and at 110 atmospheres

pressure	1 atm	110 atm		1 atm	110 atm	
composition (vol %)	melting point (°C)		ΔT(°C)	freezing point (°C)		ΔT(°C)
C_{13} (100)	-5.58	-5.29	0.29	-5.24	-3.92	1.32
C_{13} (84) C_{14} (16)	-5.63	-4.97	0.76	-4.95	-3.05	1.90
C_{13} (70) C_{14} (30)	-5.61	-5.00	0.61	-4.29	-2.34	1.95
C_{13} (60) C_{14} (40)	-5.11	-4.24	0.87	-3.50	-1.49	2.01
C_{13} (50) C_{14} (50)	-4.63	-3.92	0.71	-2.71	-0.82	1.89
C_{14} (100)	+4.56	+5.56	1.00	+6.05	+7.43	1.38

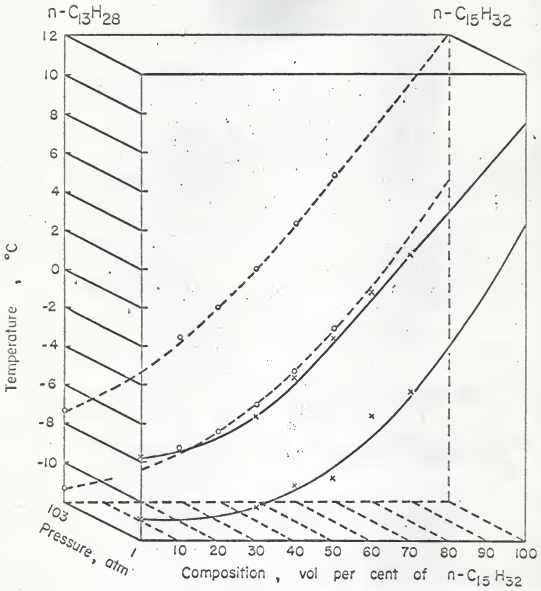

Fig.7. Phase diagrams of n-tridecane (technical grade) and n-pentadecane (technical grade) binary system.

Figure 8 shows the solid-liquid equilibrium phase diagrams of the technical grade mixture of n-tridecane and n-tetradecane. The circles represent the phase behavior at a pressure of 110 atmospheres and the crosses represent the phase behavior at a pressure of 1 atmosphere. This was plotted from Figures C-7, C-13, C-14 and C-15 in Appendix C.

Figure 9 shows the typical heating curves plotted from the potential vs. time curves of Figure C-5. A conversion table (see Appendix B) was used to convert the potential into temperature. The curve connecting the triangles represents the heating curve at a pressure of 1 atmosphere, while the curve connecting the circles represents the heating curve at a pressure of 118 atmospheres. There are two apparent breaks in both curves. The first break represents the melting point, while the second break represents the freezing point. Actual break points were determined from the round corner curves by using linear extrapolation. In other words, they were obtained by assuming that the heat capacity of the solid, that of the liquid, and the latent heat per ^{o}C remained unchanged with respect to the temperature variation in the temperature range used. The time from point A to point B corresponds to the heat required to melt the organic solution and to heat the calorimeter at the specified pressure. The time from point C to point D corresponds to the heat required to melt the organic solution and to heat the calorimeter at atmospheric pressure. Provided that the insulation condition were the same for both high pressure and low pressure operation, the relative heat of fusion of this mixture at different pressures can be estimated from the ratio of the time A to B to the time C to D.

The freezing point is considered to be the temperature at which crystals initially appear upon cooling, while the melting point is considered as that temperature at which the substance first begins to liquify upon heating. The liquidus is the curve connecting the freezing points, while the solidus is the curve connecting the melting points.

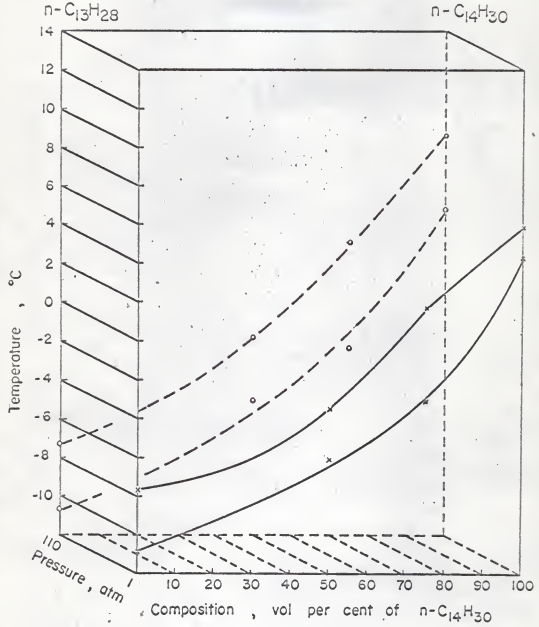

Fig. 8 . Phase diagrams of n-tridecane(technical grade) and n-tetradecane (technical grade) binary system.

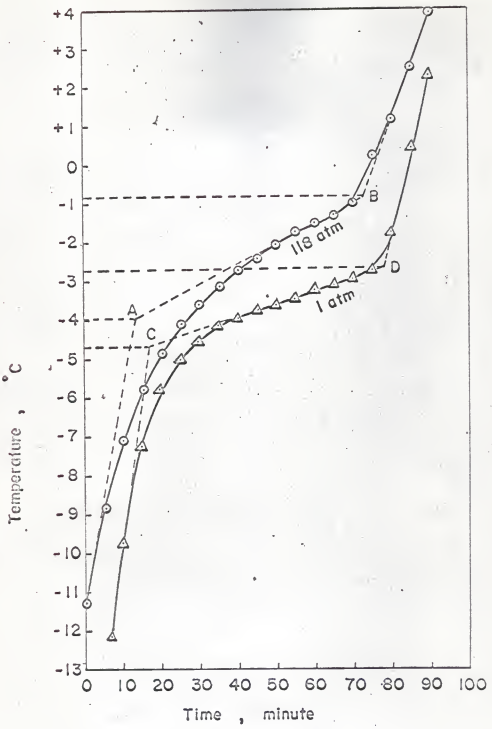

Fig. 9. Heating curves for 50 vol % n-tridecane and 50 vol % n-tetradecane (pure grade) mixture at 1 atm. and 118 atm..

Sample size did not appreciably affect the experimental results. Samples ranging from 150 ml. to 250 ml. were used.

The heat input rate may have considerable effect on the shape of the curve. A high heat input rate may result in lack of thermal equilibrium between the calorimeter and the organic solution. A slow heat input can more nearly maintain thermal equilibrium.

Generally, the e. m. f. of a thermocouple is affected by the applied pressure. However, the effect at the pressure range of 1 to 100 atmospheres can be neglected (31). Therefore, the conversion table was used both at high pressure and at atmospheric pressure without further calibration.

Volume percentage was used to express the composition in the phase diagram throughout this work. At 20 °C, the density of n-tridecane is 0.7564, the density of n-tetradecane is 0.7628, and the density of n-pentadecane is 0.7685 (32). They are nearly equal and, therefore, the volume percentage of a binary mixture of any two of these substances is approximately equal to its weight percentage.

The enthalpy of fusion increases slightly with the increase of the pressure. The enthalpy of fusion of n-tridecane at 1 atmosphere is 34.9 cal/gm and is 38.31 cal/gm at 1050 atmospheres (29); therefore, the enthalpy variation due to the pressure change under 100 atmospheres can be neglected (about 1%). The same assumption may be applied to the enthalpy of fusion of a mixture (see Figure 9) the time from A to B nearly equals to the time from C to D.

An examination of Table 3 shows that the variation of the melting point caused by the variation of pressure is smaller than the variation of the freezing point under the same conditions.

The melting point of distilled water under 1 atmosphere was measured by using the calorimeter. The result is shown in Figure 10. The horizontal straight line in Figure 10 is a reference temperature (^{o}C). The round corner of the heating curve may be due to the effect of the impurity in the water, the premelting of the ice (6), and the equivalent heat capacity of the calorimeter. From this figure, it can be seen that no overheating occurred during the experiment and the result is quite satisfactory. The melting point of distilled water was also measured at a pressure of 106 atmospheres. The result is shown in Fig. 11. The horizontal straight line in Figure 11 is a reference temperature (0^{o}C). The slope of the line connecting the melting point and the freezing point at 106 atmospheres is greater than the slope at 1 atmosphere (almost equal to zero). A melting region ranging from -0.868 ^{o}C to -0.601 ^{o}C was obtained. The average temperature is -0.74 ^{o}C. From Bridgman's data (see Appendix A), a pressure of 106 atmospheres corresponds to a melting temperature of -0.8 ^{o}C. Hence, a temperature variation of less than $\pm$0.2 ^{o}C from the real value can be predicted using this method for a single component at a pressure level of 100 atmospheres.

Curve A of Figure C-1 in the appendix, which is the heating curve of a pure grade n-tridecane under atmospheric pressure, shows that the melting region is from -5.58 ^{o}C to -5.24 ^{o}C. The average value is -5.41 ^{o}C. This coincides very well with the data cited in the Advances in Chemistry Series (32). Curve B of Figure C-1 is not very smooth, probably due to failure to maintain the ice bath at a constant temperature.

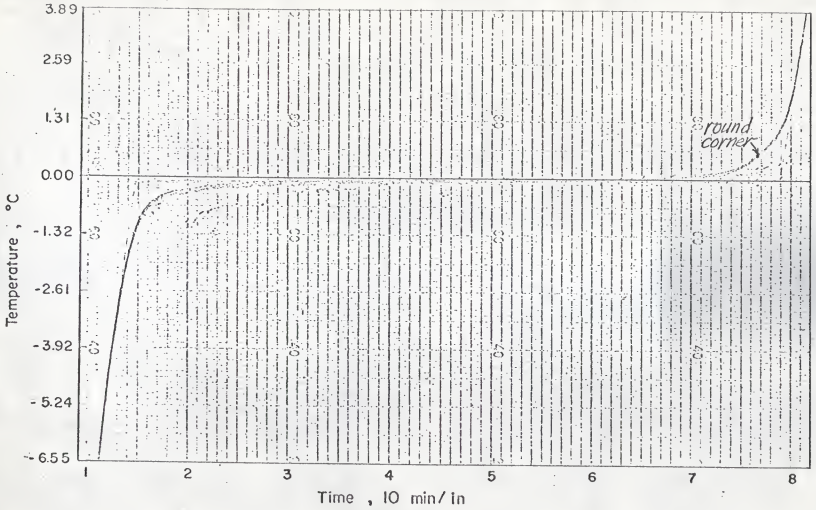

Fig. 10. Heating curve of distilled water at 1 atmosphere pressure.

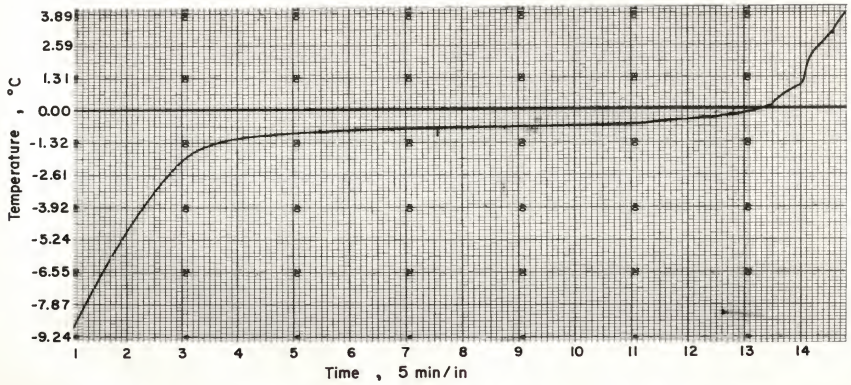

Fig. 11. Heating curve of distilled water at 106 atmosphere pressure.

Because no data are available (at the same purity of solution used in this experiment), the accuracy of measuring a mixture with the calorimeter could not be exactly extimated.

Figures 12 and 13 show the heating curves of the same mixture with a composition of 70 volume percent n-tridecane and 30 volume percent n-pentadecane (technical grade) under 103 atmospheres. By applying linear extrapolation, it can be seen that the freezing points and melting points are nearly equal. The precision of using this calorimeter to make such a measurement is within 0.1 ^{o}C.

A higher content of impurity in a sample should give rise to a larger melting region. A comparison of Figures 7 and 9 shows that the melting region of Figure 9 is larger than the melting region of Figure 6. The larger melting region corresponds to a smaller latent heat per ^{o}C. The larger the latent heat per ^{o}C the smaller the amount of refrigerant required for the process operation. Therefore, the technical grade n-tridecane and n-tetradecane and the technical grade n-tridecane and n-pentadecane systems should not be used for this inversion freezing process. The pure grade n-tridecane and n-tetradecane binary systems can be used as a refrigerant. Specifically, a composition in the neighborhood of 50 volume percent of n-tridecane and 50 volume percent of n-tetradecane is an ideal refrigerant for the inversion freezing process. Figure 14 shows the solid content vs. temperature curves plotted from Figure 6 by using the level-arm principle. For example, at a pressure of 1 atmosphere and at -4 ^{o}C and at the composition of 50 volume percent n-tridecane and 50 volume percent n-tetradecane, the ratio of solid to liquid is obtained by first drawing a straight line along the constant

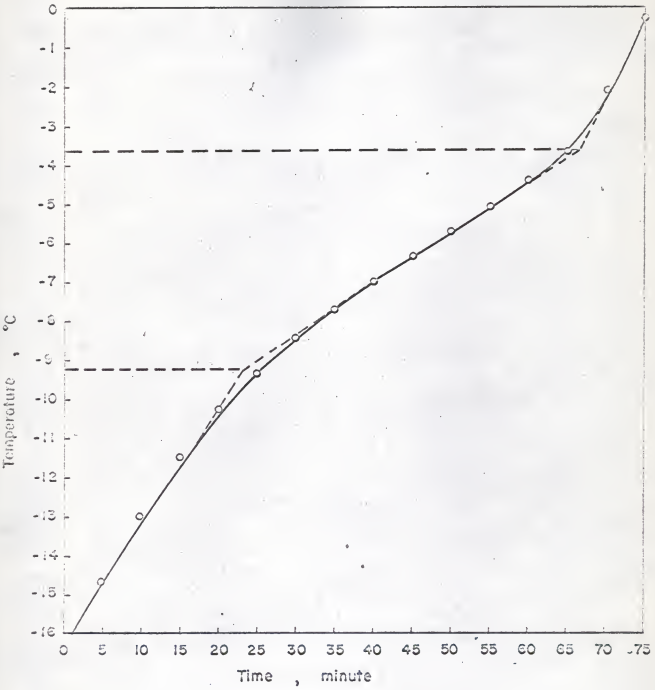

Fig.12. Heating curves for 70 vol % n-tridecane and 30 vol % n-pentadecane (technical grade) mixture at 103 atm. (run 1).

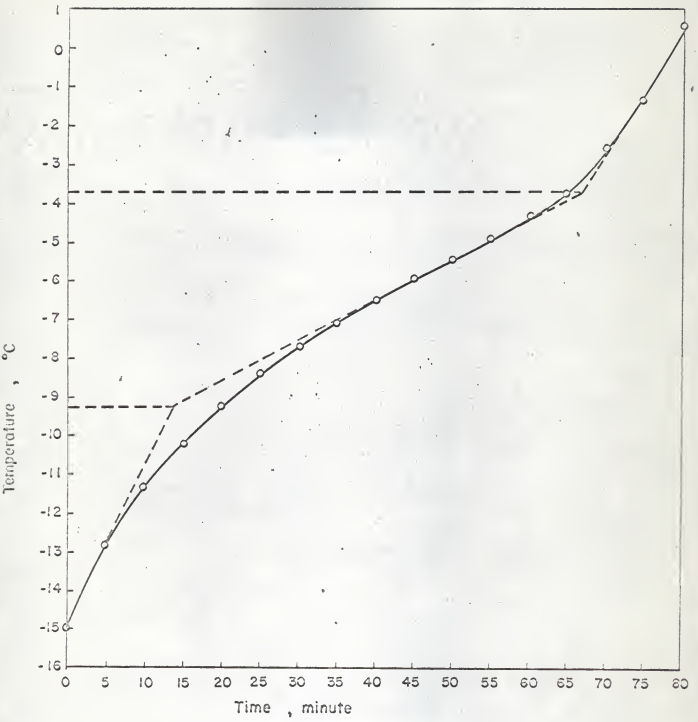

Fig. 13. Heating curves for 70 vol % n-tridecane (pure grade) and 30 vol % n-pentadecane (technical grade) mixture at 103 atm (run 2).

temperature axis and a straight line along the constant composition axis and then taking the ratio of the distance between liquidus and the constant composition line to the distance between the constant composition line and the solidus. Figure 14 can be used for process design for the inversion freezing process.

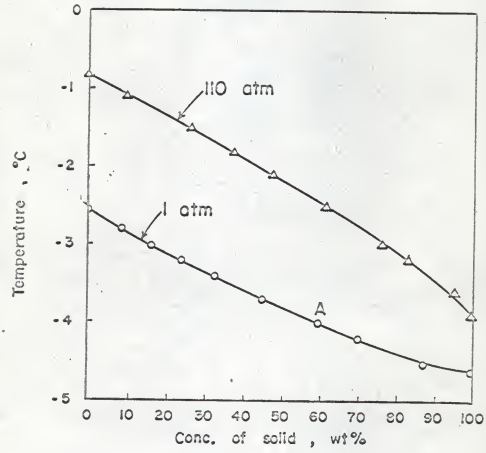

Fig.14. Solid content vs. temperature of a mixture of 50 vol % n-tridecane (pure grade) and 50 vol % n-tetradecane (pure grade) at 1 atm and 110 atm .

LITERATURE CITED

1. Muller, J. G., Chem. Engg. Prog. 59, No. 12 (December 1963).

2. Cheng, C. Y., and S. W. Cheng, A. I. Ch. E. J. 13, 41 (1967).

3. Ricci, J. E., "Phase Rule and Heterogeneous Equilibrium," p. 30, Nostrand, New York (1951).

4. Bridgman, P. W., "International Critical Tables," 4, 11, McGraw-Hill, New York (1928).

5. Skau, E. L., J. C. Arthur and H. Wakeham, in Technique of Organic Chemistry 1, Interscience, New York (1965).

6. Cines, M. R., in Physical Chemistry of Hydrocarbons 1, A. Farkas, ed., Academic Press, Inc., Publishers, New York (1950).

7. Westrum, E. F., Jr., and J. P. McCullough, in Physical and Chemistry of the Organic Solid State, 1, D. Fox, M. M. Labes and A. Weissberger, eds., Interscience Publishers, New York (1963).

8. Stull, D. R., J. Am. Chem. Soc. 59, 2726 (1937).

9. Aston, J. G. and M. L. Eidinoff, J. Am. Chem. Soc. 61, 1533 (1939).

10. Ziegler, W. T., and C. E. Messer, J. Am. Chem. Soc. 63, 2694 (1941).

11. Ruehrwein, R. A., and H. M. Huffman, J. Am. Chem. Soc. 65, 1620 (1943).

12. Tilicheev, M. D., V. P. Peshkov, and S. A. Yuganova, J. Gen. Chem. 21, 1341 (1951).

13. Finke, H. L., M. E. Gross, G. Waddington, and H. M. Huffman, J. Am. Chem. Soc. 76, 333 (1953).

14. Salzgerber, M. R., Academie Des Sciences 18, 1642 (1955).

15. Tunnicliff, D. D., and H. Stone, Ana. Chem. 27, 73 (1955).

16. Aranow, R. H., L. Witten, and D. H. Andrews, J. Phys. Chem. 62, 812 (1958).

17. Vassallo, D. A., and J. C. Harden, Ana. Chem. 34, 132 (1962).

18. Schwab, F. W., and E. Wichers, in Temperature, Its Measurement and Control in Science and Industry, Reinhold, New York , p. 256 (1941).

19. Smittenberg, J., H. Hoog, and R. A. Henkes, J. Am. Chem. Soc. 60, 17 (1938).

LITERATURE CITED--Continued

20. Skau, E. L., Proc. Am. Acad. Arts Sci., 67, 551 (1933).

21. Glasgow, A. R., Jr., A. J. Streiff, and F. D. Rossini, J. Research Natl. Bur. Standards, 35, 355 (1945).

22. Aston, J. G., H. L. Fink, C. T. Hardwick, and C. F. Salzman, presented at Chicago Meeting, Am. Chem. Soc., (April, 1946).

23. Aston, J. G., H. L. Fink, J. W. Tooke, and M. R. Cines, Ind. Eng. Chem., Anal. Ed., 19, 218 (1947).

24. Southard and Brickwedde, J. Am. Chem. Soc. 55, 4378 (1933).

25. Andrews, J. Am. Chem. Soc., 48, 1287 (1926).

26. Blue and Hicks, J. Am. Chem. Soc. 59, 1962 (1937).

27. Bridgman, P. W., The Physics of High Pressure, G. Bella and Sons, Ltd. (1949).

28. Cutler, W. G., R. H. McMickle, W. Webb, and R. W. Schiessler, J. Chem. Phy. 29, No. 4, 727 (1958).

29. Nelson, R. R., W. Webb, and J. A. Dixon, J. Chem. Phy. 33, No. 6, 1756 (1960).

30. Autoclave Engineers, "Catalog and Handbook," Bulletin 1051-C, p. 3 (1959).

31. Klement, W. Jr., and A. Jayaraman, in "Progress in Solid State Chemistry," Reiss H., ed., 3, 289, Pergamon Press, Inc. (1967).

32. Physical Properties of Chemical Compounds-II, pp. 164-166, American Chemical Society, Washington D. C. (1959).

ACKNOWLEDGMENTS

The author wishes to express his sincere gratitude to his major advisor, Dr. Liang-Tseng Fan for his constant advice and guidance in this study. The author also expresses his gratitude to Dr. Richard G. Akins and Dr. Chen-Yen Cheng for their suggestions and assistance.

The financial support of this work from Kansas State University Engineering Experiment Station project 2434, supported by the Office of Saline Water, is also acknowledged.

APPENDIX A

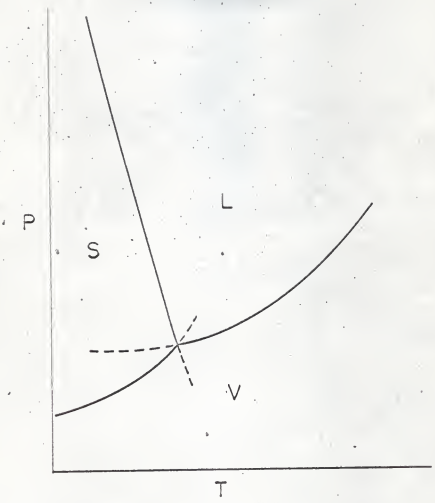

Fig. A-1: Pressure vs. temperature curve of water (schematic).

Table A-1. Melting Points of Water at Different Pressures

P, atm	T, °C
1	0.0
590	-5.0
1090	-10.0
1540	-15.0
1910	-20.0

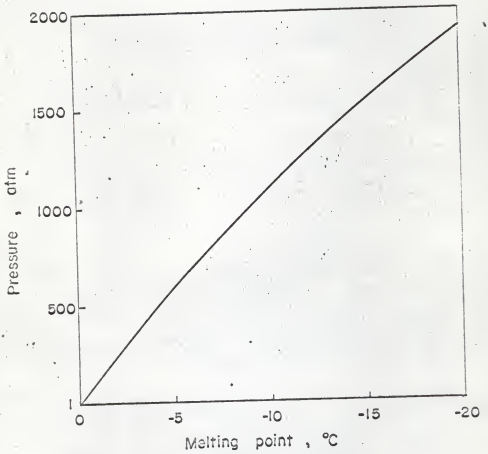

Fig. A-2. Melting point vs. pressure curve of water.

APPENDIX B

Table B-1. Potential and Temperature Conversion Table

Copper vs. Constantan Thermocouple
Degrees Centigrade Reference Junction 0° C.

°C	0	1	2	3	4	5	6	7	8	9
						Millivolts				
-50	-1.804	-1.838	-1.871	-1.905	-1.938	-1.971	-2.004	-2.037	-2.070	-2.103
-40	-1.463	-1.498	-1.532	-1.567	-1.601	-1.635	-1.669	-1.703	-1.737	-1.771
-30	-1.112	-1.148	-1.183	-1.218	-1.254	-1.289	-1.324	-1.359	-1.394	-1.429
-20	-0.751	-0.788	-0.824	-0.860	-0.897	-0.933	-0.969	-1.005	-1.041	-1.076
-10	-0.380	-0.417	-0.455	-0.492	-0.530	-0.567	-0.604	-0.641	-0.678	-0.714
(-)0	0.000	-0.038	-0.077	-0.115	-0.153	-0.191	-0.229	-0.267	-0.305	-0.343
(+)0	0.000	0.038	0.077	0.116	0.154	0.103	0.232	0.271	0.311	0.350
10	0.389	0.429	0.468	0.508	0.547	0.587	0.627	0.667	0.707	0.747
20	0.787	0.827	0.868	0.908	0.949	0.990	1.030	1.071	1.112	1.153
30	1.194	1.235	1.277	1.318	1.360	1.401	1.443	1.485	1.526	1.568
40	1.610	1.652	1.694	1.737	1.779	1.821	1.864	1.907	1.949	1.992

APPENDIX C

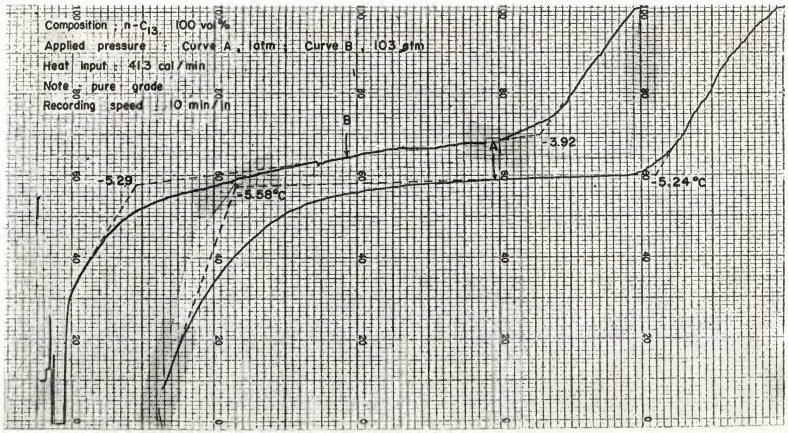

Fig. C-1. Heating curves of a pure grade n-tridecane($n\text{-}C_{13}H_{28}$) under 1 atm and 103 atm.

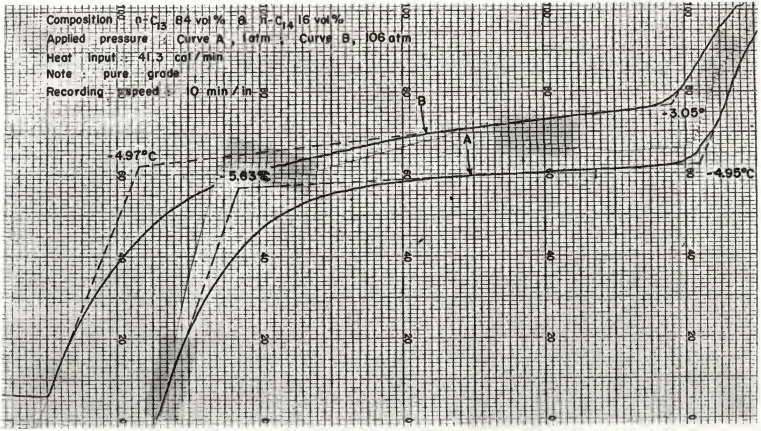

Fig. C-2. Heating curves of a mixture of n-tridecane ($n\text{-}C_{13}H_{28}$) (84 vol %) and n-tetradecane ($n\text{-}C_{14}H_{30}$) (16 vol %), (pure grade) under 1atm and 106 atm.

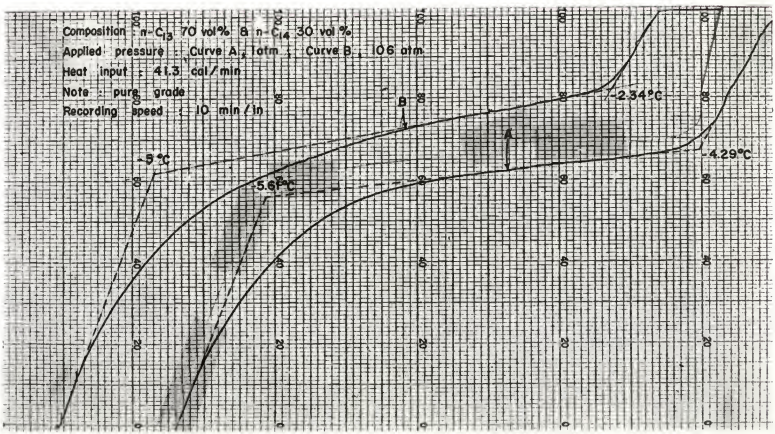

Fig. C-3. Heating curves of a mixture of n-tridecane($n\text{-}C_{13}H_{28}$)(70vol%) and n-tetradecane($n\text{-}C_{14}H_{30}$)(30vol%), (pure grade) under 1atm and 106 atm.

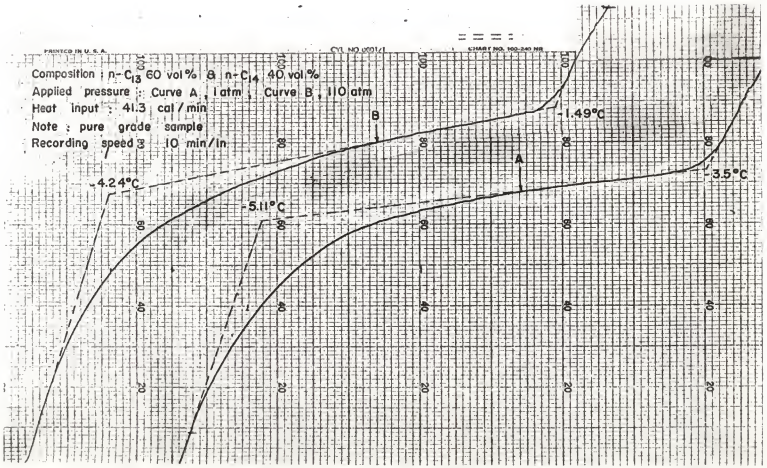

Fig. C-4. Heating curves of a mixture of n-tridecane(n-$C_{13}H_{28}$)(60 vol %) and n-tetradecane(n-$C_{14}H_{30}$)(40 vol %), (pure grade) under 1 atm and 110 atm.

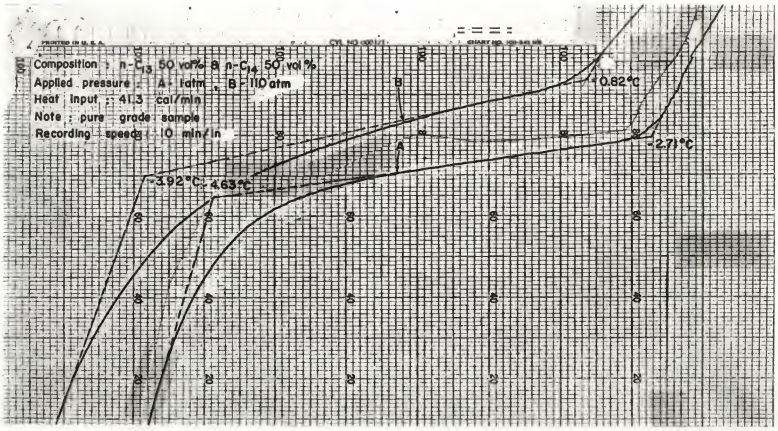

Fig. C-5. Heating curves of a mixture of n-tridecane($n\text{-}C_{13}H_{28}$)(50 vol %) and n-tetradecane($n\text{-}C_{14}H_{30}$)(50 vol %),(pure grade) under 1 atm and 110 atm.

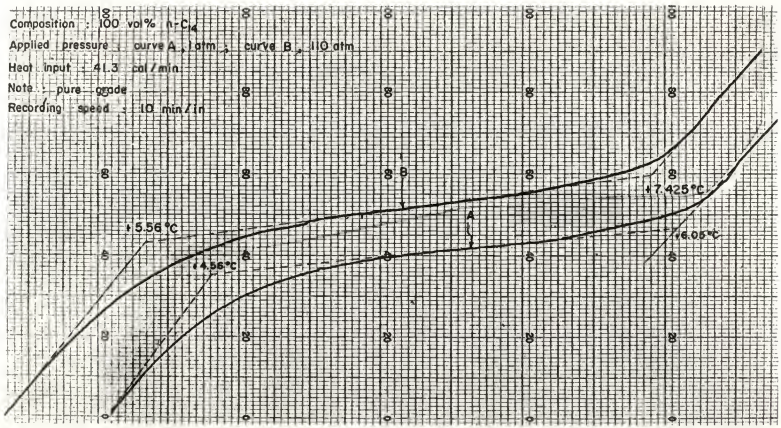

Fig. C-6. Heating curves of a pure grade n-tetradecane ($n\text{-}C_{14}H_{30}$) under 1 atm and 110 atm.

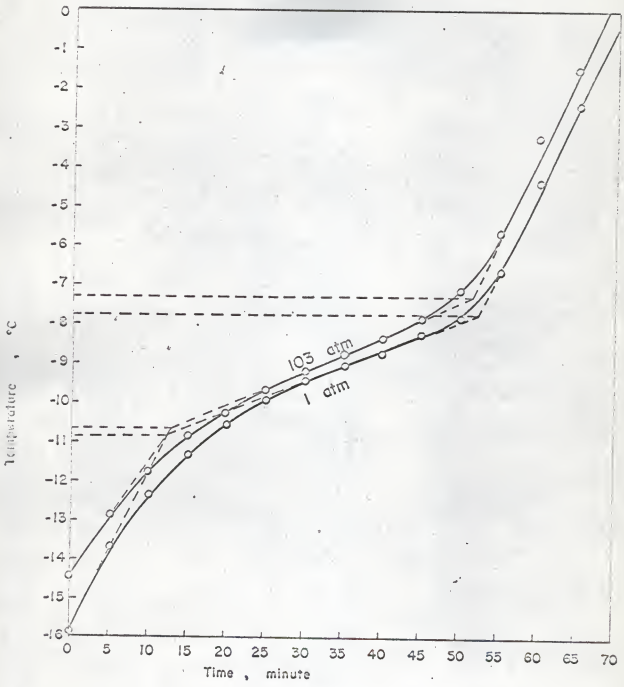

Fig. C-7. Heating curves of technical grade n-tridecane under 1 atm and 103 atm.

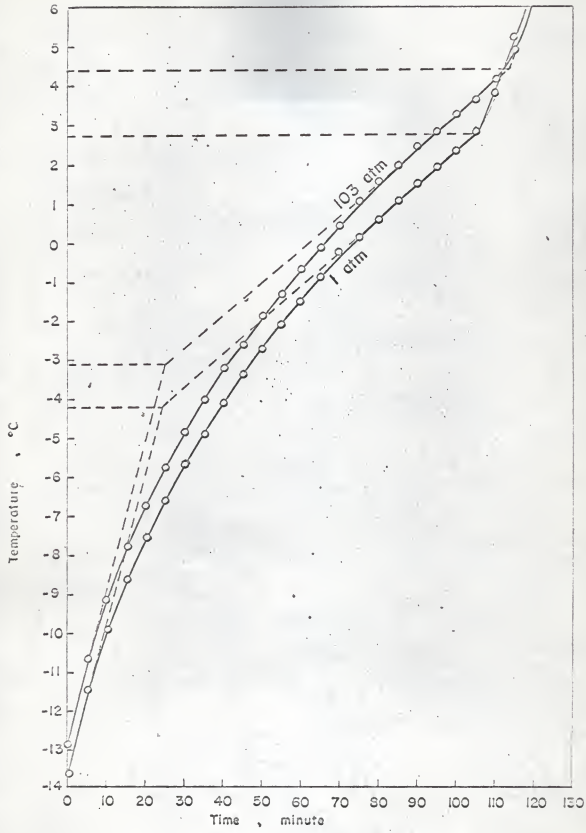

Fig. C-8. Heating curves of a mixture of n-tridecane ($n\text{-}C_{13}H_{28}$) (30 vol %) and n-pentadecane ($n\text{-}C_{15}H_{32}$) (70 vol %), (technical grade) under 1 atm and 103 atm.

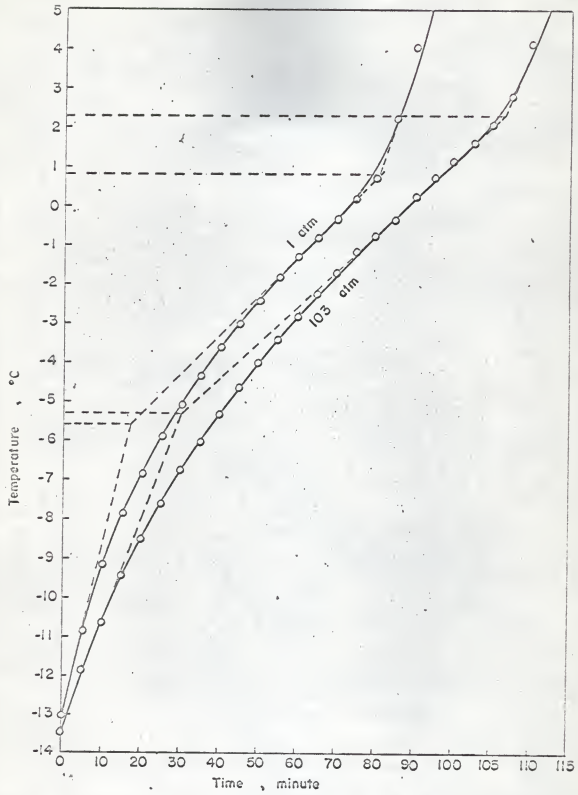

Fig. C-9. Heating curves of a mixture of n-tridecane ($n\text{-}C_{13}H_{28}$) (40 vol %) and n-pentadecane ($n\text{-}C_{15}H_{32}$) (60 vol %) (technical grade) under 1 atm and 103 atm.

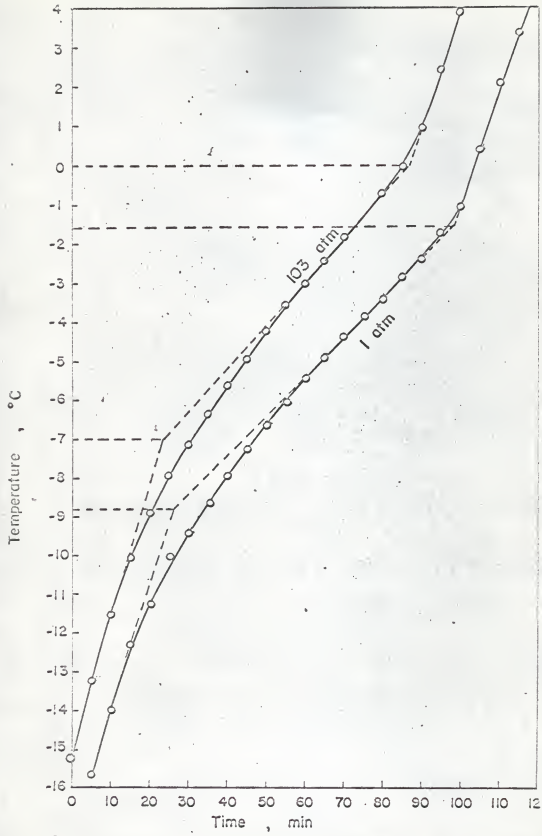

Fig. C-10. Heating curves of a mixture of n-tridecane (n-$C_{13}H_{28}$) (50 vol %) and n-pentadecane(n-$C_{15}H_{32}$) (50 vol %),(technical grade) under 1atm and 103 atm.

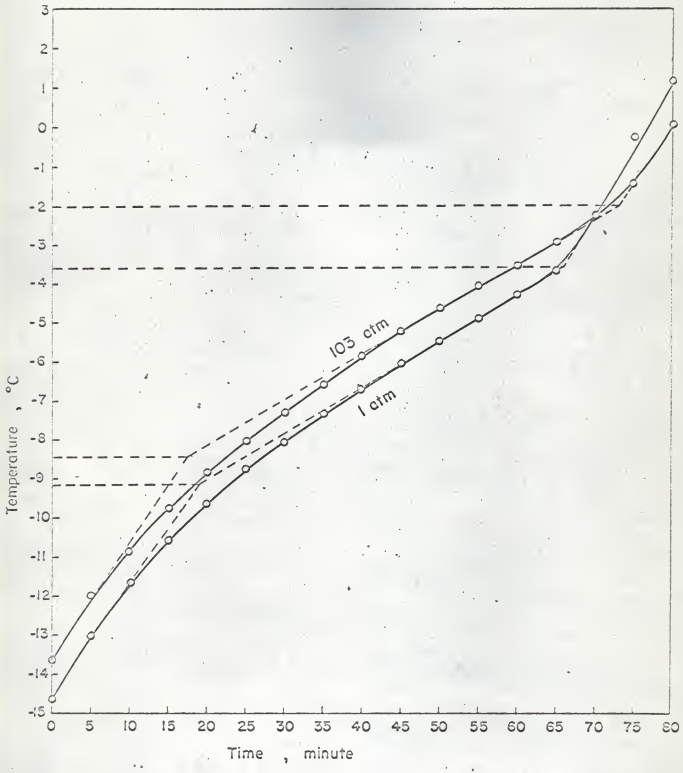

Fig. C-11. Heating curves of a mixture of n-tridecane ($n-C_{13}H_{28}$)(60 vol%) and n-pentadecane ($n-C_{15}H_{32}$)(40 vol %) (technical grade) under 1 atm and 103 atm.

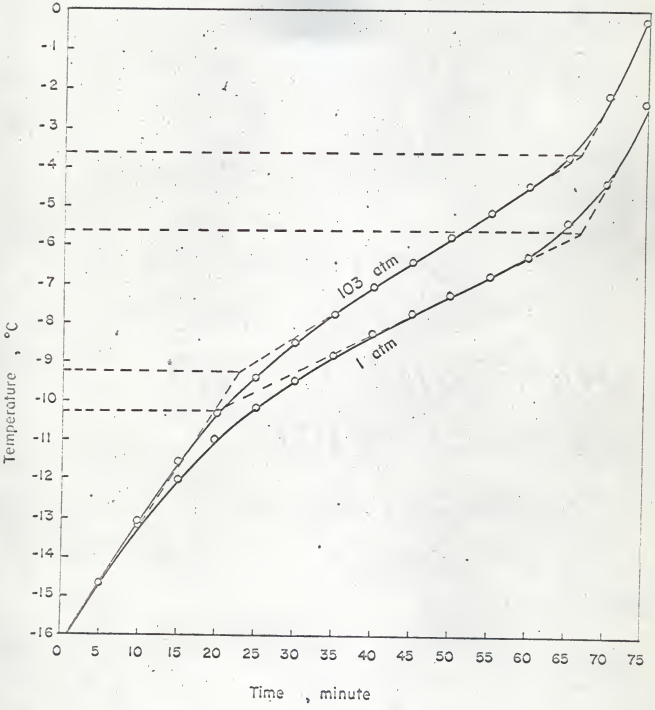

Fig. C-12. Heating curves of a mixture of n-tridecane (n-$C_{13}H_{28}$) (70 vol %) and n-pentadecane (n-$C_{15}H_{32}$) (30 vol %), (technical grade) under 1 atm and 103 atm.

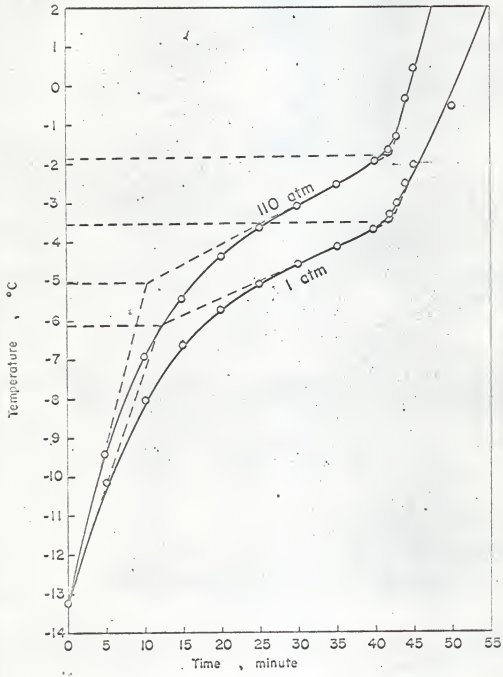

Fig. C-13. Heating curves of a mixture of n-tridecane ($n\text{-}C_{13}H_{28}$) (50 vol %) and n-tetradecane ($n\text{-}C_{14}H_{30}$) (50 %), (technical grade) under 1 atm and 110 atm.

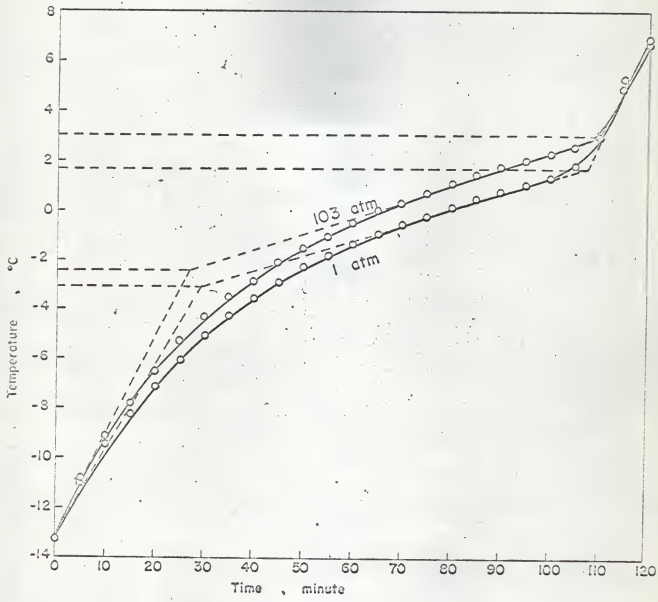

Fig. C-14. Heating curves of a mixture of n-tridecane ($n\text{-}C_{13}H_{28}$) (25 vol%) and n-tetradecane ($n\text{-}C_{14}H_{30}$) (75 vol%), (technical grade) under 1 atm and 103 atm.

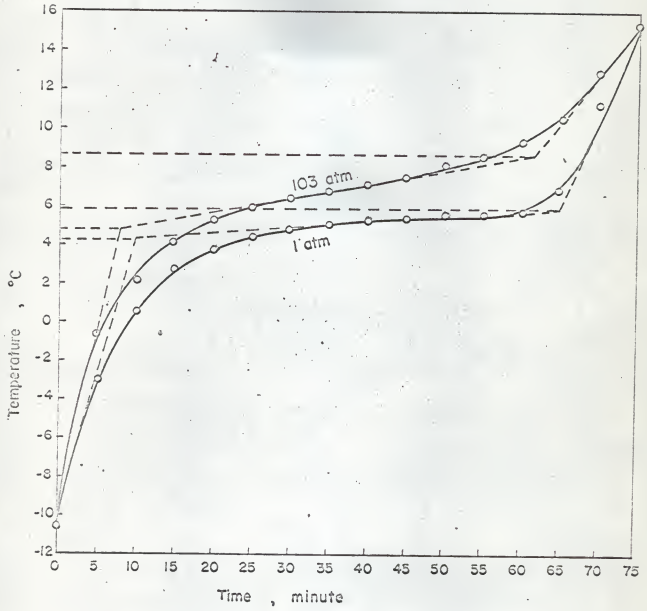

Fig. C-15. Heating curves of technical grade n-tetradecane (n-$C_{14}H_{30}$) under 1 atm and 103 atm.

PHASE DIAGRAM STUDIES OF BINARY HYDROCARBON SYSTEMS FOR A FREEZING DESALINATION PROCESS

by

PETER SHENG-SHYONG MAA

B. S., National Taiwan University, 1964

AN ABSTRACT OF A MASTER'S THESIS

submitted in partial fulfillment of the

requirements for the degree

MASTER OF SCIENCE

Department of Chemical Engineering

KANSAS STATE UNIVERSITY
Manhattan, Kansas

1968

Experimental equipment was designed and built for measuring the phase diagrams of binary hydrocarbon systems within the pressure range of 0 psig to 2000 psig. A calorimeter was devised to maintain thermo-equilibrium to obtain the solid-liquid equilibrium temperature to within 0.2 °C.

Three binary hydrocarbon systems were measured; one was the n-tridecane (pure grade) and n-tetradecane (pure grade) binary system; another was the n-tridecane (technical grade) and n-pentadecane (technical grade) binary system, and the last one was the n-tridecane (technical grade) and n-tetradecane (technical grade) binary system. Six phase diagrams were obtained. Three were at atmospheric pressure. The others were at 100 to 110 atmospheres.

From these phase diagrams, a comparison was made of the properties of the solutions as refrigerants for the inversion freezing process. The best solution appeared to be 50 volume percent n-tridecane and 50 volume percent n-tetradecane (pure grades). A plot of the solid content (fraction frozen) vs. temperature at latm. and at 110 atm. of this solution was made. This can be used for the design of the ice maker and the high-pressure ice melter for the inversion freezing process.